

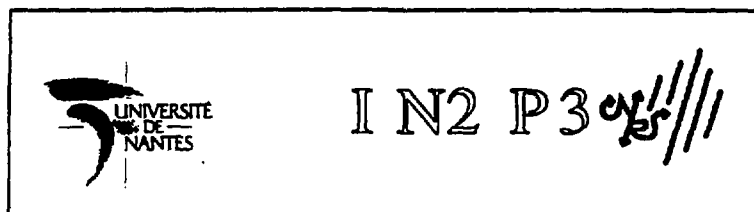


IR9401519

LABORATOIRE DE PHYSIQUE NUCLEAIRE

UNITE ASSOCIEE AU CNRS/IN2P3 (UA 57)

2, rue de la Houssinière 44072 NANTES CEDEX 03



STUDY OF ENERGY DEPOSITION IN HEAVY-ION REACTIONS

V. De La Mota, F. Sébille, P. Abgrall, F. Haddad

Rapport Interne LPN - 93-04

UNIVERSITE DE NANTES

Study of energy deposition in heavy-ion reactions

P. Abgrall, F. Haddad, V. de la Mota, F. Sébille

Laboratoire de Physique Nucléaire, Université de Nantes-*IN₂P₃*.

F-44072 Nantes Cedex 03. France.

Abstract

An investigation of energy deposition mechanisms in heavy-ion reactions at intermediate energies is presented. Theoretical simulations are performed in the framework of the semi-classical Landau-Vlasov model. They emphasize the influence of the initial non-equilibrium conditions, and the connection with the incident energy is discussed. Characteristic times involved in the energy thermalization process and finite size effects are analyzed.

PACS numbers: 25.70-z

Heavy ion collisions at intermediate energies represent currently a useful tool devoted to the study of excited and hot nuclear matter properties. Among the main motivations of these investigations are the characterisation of the nuclear equation of state and the determination of the maximum temperature that a nucleus can sustain without dissociating. Nevertheless, this purpose is not obvious since the equation of state (EOS) and temperature are concepts only well defined at equilibrium. In particular, the nuclear EOS is defined in infinite nuclear matter, and most of the EOS properties of finite nuclei have been

largely studied near their ground state [1]. In this sense, heavy-ion reactions at intermediate energies can provide interesting informations about the properties of excited nuclear matter far away from equilibrium [2].

Recent experiments suggested a limiting temperature, of about 5 MeV for different reactions [3,4]. However, further experiments concerning violent collisions between very heavy systems, showed that nuclei can be found more excited [5,6] at beam energies of few tens MeV per nucleon. In addition, it has been shown [7] that compact thermalized residues produced in heavy-ion reactions can saturate around 7 MeV of temperature. These apparently contradictory results constitute a motivation for microscopic theoretical models to better understand the experimental data and gain new insights in the study of the reaction mechanisms in hot nuclei. It is well known that temperatures and excitation energies are not directly measured but determined by experimental models, where in general dynamical aspects are not present. Confrontation with data could throw light on the role played by these models and the experimental biases, as detection thresholds, in the results obtained.

A certain number of theoretical works were focused in this direction [8-10] involving different criteria for the characterization of the thermalization process. The aim of this work is to present the main technical aspects of our theoretical approach for the evaluation of the deposited energy in a nuclear reaction, based on the Landau-Vlasov model [11,12]. This paper does not intend to give a systematic analysis of the limiting temperature problem in hot nuclei, but rather a discussion of the basic assumptions concerning the definition and calculation of relevant observables. An analysis in terms of effective forces and the interpretation of quantitative results in closer connection with experimental data will be presented in a further work [13].

Let us briefly recall the Landau-Vlasov equation giving the time evolution of the one body distribution function in phase space $f(\vec{r}, \vec{p})$:

$$\frac{\partial f}{\partial t} + \{f, H\} = I_{\text{coll}}(f) \quad , \quad (1)$$

where $\{ , \}$ stands for the Poisson bracket, H is the one-body Hamiltonian and $I_{\text{coll}}(f)$ is the collision integral calculated in the Uehling-Uhlenbeck approximation. This collision term reads:

$$I_{\text{coll}} = \frac{g}{4m^2} \frac{1}{\pi^3 \hbar^3} \int d\vec{p}_2 d\vec{p}_3 d\vec{p}_4 \frac{d\sigma}{d\Omega} \delta(\vec{p} + \vec{p}_2 - \vec{p}_3 - \vec{p}_4) \delta(p^2 + p_2^2 - p_3^2 - p_4^2) \\ \times \{ (1 - \bar{f})(1 - \bar{f}_2)f_3f_4 - (1 - \bar{f}_3)(1 - \bar{f}_4)f_2f \} \quad , \quad (2)$$

here σ is the free nucleon-nucleon cross-section, with its usual energy and isospin dependence, $\bar{f} = (2\pi\hbar)^3 f(\vec{r}, \vec{p})/g$ is the occupation number, and g is the degeneracy. This equation is solved for a local effective force of the Skyrme type [11] by expanding the Wigner function $f(\vec{r}, \vec{p})$ on a basis of coherent states:

$$f(\vec{r}, \vec{p}) = \frac{A}{N} \sum_i \omega_i g_x(\vec{r} - \vec{r}_i) g_\phi(\vec{p} - \vec{p}_i) \quad (3)$$

which follow semi-classical trajectories in phase space [11,12]. In this last equation A is the mass number, N is the number of coherent states, actually a basis of gaussians, and the w_i are weight factors [9]. According to Ref. [14], the ratio N/A has been fixed in order to minimize fluctuations in global observables. This corresponds to about 40 gaussians per nucleon in our particular case.

Let us now define the energy transfers between microscopic and macroscopic degrees of freedom in our semi-classical model. A local collective current is defined as follows¹:

¹integrals are here extended in all phase-space.

$$\vec{J} = \rho \vec{v} = \int \frac{\vec{p}}{m} f(\vec{r}, \vec{p}) d\vec{p} \quad (4)$$

ρ being the local density:

$$\rho(\vec{r}) = \int f(\vec{r}, \vec{p}) d\vec{p} \quad (5)$$

If we take $\vec{p} = p_{lab} - P_{CM}$, the collective kinetic energy in the center of mass frame is given by:

$$E_{coll} = \frac{1}{2} \int \frac{J^2(\vec{r})}{\rho(\vec{r})} d\vec{r} \quad (6)$$

Calling E_k and E_0 the total and the “cold” internal kinetic energy, respectively, the excitation energy of the complete system E^* can be defined as:

$$E^* = E_k - E_{coll} - E_0 \quad (7)$$

In semiclassical models one common way to estimate E_0 is in the Thomas-Fermi limit, which represents the kinetic energy contained in a spherical momentum distribution function. This approximation, in principle valid for infinite homogeneous nuclear matter at equilibrium, has been adapted to finite systems taking into account the surface and the potential gradients through the local density [15]. In the common Thomas-Fermi approximation, that for sake of simplicity we call here Local Sphere Approximation (L.S.A.), the cold internal

kinetic energy reads:

$$E_0 = \frac{\hbar^2}{2m} \frac{5}{3} \left(\frac{3}{2} \pi^2 \right)^{\frac{2}{3}} \int \rho(\vec{r})^{\frac{2}{3}} d\vec{r} \quad (8)$$

However, in heavy-ion reactions at intermediate energies the momentum distribution is far from being spherical, at least during the initial stages of the collision. This initial non-equilibrium configuration can be characterized through the quadrupole moment in coordinate \vec{p} :

$$Q_{zz}(\vec{r}) = \int (2p_z^2 - p_x^2 - p_y^2) f(\vec{r}, \vec{p}) d\vec{p} \quad (9)$$

In this spirit, the initial momentum distribution of two colliding nuclei is simply simulated by two Fermi spheres [16,17] separated by a distance ϵ in the direction of the beam axis which represents their relative momentum (see Fig. 1). The radii of the spheres and ϵ are determined iteratively from the true local density and local quadrupole moment. In this approximation:

$$\rho(\epsilon, k_F) = \frac{g}{(2\pi)^3} V k_F^3 \quad (10)$$

$$Q_{zz}(\epsilon, k_F) = \eta \frac{k_F^2}{V} \quad (11)$$

where $\hbar k_F$ is the Fermi momentum and V and η are, respectively, the volume of the momentum distribution and a factor coming from the integration over \vec{p} in equation (9). Both quantities depend on the ratio ϵ/k_F . Due to the

saturation of nuclear force at equilibrium we have chosen the same radius for the two spheres in a symmetric system. The “cold” kinetic energy is calculated for two sharp Fermi surfaces, in the same way as in the Thomas Fermi limit, which is recovered making ϵ tend to 0. We will call this approach the Local Bisphere Approximation (L.B.A.). More sophisticated descriptions of the non-equilibrium distribution can be introduced namely including different spheres radii [17] or surface diffuseness. The present simplified version has been chosen in order to describe symmetric systems, keeping our numerical calculations within reasonable margins of computing time.

The validity of such approximations can be tested through numerical simulations in particular cases in which a well defined behavior in the excitation energy is expected. Let us first define a residue at each time step as the part of the colliding system for which the spatial density is higher than the threshold $\rho_{max}/10$. The observables previously defined can be calculated, in this case, by limiting the integrals in eqs. 4 - 9 to the phase space region involved by the residue. The estimation of the excitation energy strongly depends on the way E_0 is calculated. Indeed, Fig. 2 reports this quantity as a function of time in the (Ca 60MeV/A)+ Ca head-on collision in different dynamical situations. The dotted and dashed lines represent the excitation energy of the residue in the L.S.A. and L.B.A., respectively. Aiming at minimizing the contribution of thermal intrinsic degrees of freedom we have turned off the two nucleon collisions and plotted the same quantity in the bisphere approximation (solid line). In this case, apart from the values in the long times tail, the results extracted in the L.S.A. are similar to those obtained when two-body collisions are included, and for this reason they are not plotted.

We have to mention that the estimated excitation energy is initially non negligible and that it can decrease under the initial value in the most dilute phases of the reaction. Both effects are consequences on one hand of the numerical approximations made to evaluate equation (8), and on the other hand

of the fact that the cold kinetic energy E_0 is calculated at the lowest order in a semi-classical expansion of the potential [18] in the extended Thomas-Fermi point of view. These combined effects introduce a shift with respect to the zero of the thermal excitation energy. It shall also be seen further that in some cases the asymptotic value of the excitation energy can be smaller than the initial one, which is consistent with the loss of mass of the residues. But beyond this aspect, comparing dotted and solid lines it clearly appears that if the initial non-equilibrium distribution is not taken into account a spurious amount of excitation coming from the momentum distribution, contributes to the total thermal energy.

When two-body collisions are included their role is to allow the thermalization of the system, this fact depending on the reaction time scales. We are concerned then with the concept of a thermal equilibration time that we choose as the time at which the total momentum distribution becomes locally spherical. In other words, at a given point in the configuration space and at $t = t_e$ the local Fermi bisphere becomes a single sphere and the system can be considered in local equilibrium. In Fig. 2 the equilibration time obtained when two-body collisions are allowed is pointed with an arrow. The excitation energy evaluated for the residue at the time t_e can be considered as the maximum thermalised energy which has been deposited in the system.

Our characteristic time of thermalization t_e differs from that of Ref. [10], where it is defined as the time for which the excitation energy exhibits a second maximum, and it was called the freeze-out time t_f . As we shall see this second peak does not always exist, depending on the characteristics of the entrance channel. This is the case for the particular reaction with a beam energy of 60 MeV per nucleon, where the residue breaks up completely in the final state.

With our definition of t_e it is possible to estimate the energy drained by the so-called pre-equilibrium particles. In Figs. 3 we represent for a Ca on Ca collision at 40 and 60 MeV/n the internal excitation energy of the residue E_{int}^*

(solid line), the emitted particles energy plus E_{int}^* (dashed-dotted line) and the sum of this quantity and the collective energy (dashed line). The difference between the horizontal straight line, representing the initial kinetic energy, and the dashed line corresponds to the variation of the potential energy plus the cold kinetic energy. Two different regimes get clear. Effectively, in Fig. 3.a it appears that the calculated maximum thermalized energy is recovered by the energy carried away by the evaporated particles. Nevertheless, for the lower beam energy the final residue deexcites passing through various compression-decompression stages, represented by oscillations in the excitation energy, which are more marked than for the higher energy. Due to these oscillations, which characterize exchanges between different energy contributions, the connection between the maximum deposited energy and the characteristics of the detected particles is not direct. In fact, we can see in Fig. 3b that for times greater than t_e , the system evaporates releasing energy until it attains a dilute phase, after which it tends to recontract itself again, passing through a new compressed stage. This corresponds to the second peak in the plot of $E_{int}^*(t)$. It can be seen in this case that at times around 400 Fm/c the residue has completely decayed and the resulting "evaporated" energy is higher than $E_{int}^*(t_e)$.

We must stress here on the fact that in this case the deposited energies estimated at t_f or t_e are of the same order, the difference being in the definition of the thermalized regime. This model calculation poses the problem of the experimental signatures and their connection with the temperature concept, since in addition, pre-equilibrium as well as finite size effects play a significant role in the dynamical processes of energy transfer, in either collective or intrinsic degrees of freedom. Whatever the incident energy is, a large amount of excitation energy is deposited in the intrinsic degrees of freedom during the early stages of the reaction, and a significant part of it is already carried out by the emitted particles before an isotropic distribution takes place in the momentum space. The transition from anisotropy to isotropy is continuous, and a precise splitting

between pre-equilibrium and evaporated particles cannot be completely figured out. Nevertheless, in the cases displayed in Figs. 3, the thermalization is always reached during a stage of the reaction where the colliding system is still compact, and before it enters the exit channel leading either to the breaking of the system or to a heavy residue.

Let us finally see what kind of information we can get from the analysis of relaxation time scales, which have been shown to be of crucial importance in the explanation of experimental data [7]. The relaxation of the Fermi bisphere determines a specific time scale which characterizes the thermalization process of the system and that can be estimated from the time evolution of certain observables. Indeed, the difference between the excitation energy evaluated in the local bisphere approximation and its equilibrated value decreases in time in an approximative exponential way. A local relaxation time τ can then be defined as the decay parameter of the approximated exponential function, in concordance with the usual definition of the global relaxation time τ_Q of the total quadrupole moment. Let us simply recall that since these parameters are extracted from the evolution of mean values of observables governed by the Landau-Vlasov dynamics, they are the result of combined gain-minus-loss processes in phase space. Complementary informations can be found in Ref. [19]. In Fig. 4 the relaxation time τ is plotted as a function of the incident energy for the Ca+Ca and Pb+Pb central collisions, in dashed-dotted and dotted lines, respectively. We also show the results obtained for τ_Q for the Pb+Pb reaction in solid line. We observe that these characteristic times are decreasing functions of the energy except for the light system, for which τ is nearly constant. In this case, the relaxation is faster than for the heavier system, which is less diffuse and the accessible phase space via two-body collisions is more blocked, mainly in the compressed stages. We must stress here the fact that the energy independence of τ found in the Ca+Ca system was already pointed out in Ref. [20] in the framework of a quantal phase space description. Our results are of

the same order of magnitude as those obtained in the mentioned work for the Ca+Ca reaction.

Summarizing, in this work we showed the importance of considering the initial non equilibrium momentum distribution in the calculation of the excitation energy in nuclear collisions at intermediate energies. If this dynamical aspect is neglected the excitation energy is overestimated. In this context, we proposed a criterium to evaluate the deposited energy in the nuclear system in the framework of the Landau Vlasov model. This criterium concerns the determination of the equilibration time t_e , the time at which the momentum distribution attains a single spherical shape. The theoretical determination of t_e is somewhat delicate because of the rapid variation of the phase space configuration during the interpenetration of the colliding system. In this sense, for a quantitative analysis it is more adequate to deal with an uncertainty interval around t_e rather than with t_e itself. Characteristic time scales were extracted from the time evolution of the local excitation energy and the global quadrupole moment. Local thermalization seems to be attained faster for small systems and nearly independently of the incident energy. The crucial question here is to find adequate observables to provide informations about the "thermalized" deposited energy knowing that the interplay between thermal and compression contributions may play an important role in the reaction dynamics. In order to better understand the critical behaviour of hot and excited nuclear matter, an extensive analysis concerning a variety of systems, asymmetries and energies is necessary, in the same way as in experimental grounds. This study is now in progress and will be further reported.

References

- [1] J.P. Blaizot, Phys. Rep. **64C** 171 (1980); and references therein.
- [2] V. de la Mota, F. Sébille, B. Remaud and P. Schuck, Phys. Rev. **C46** 667 (1992)
- [3] D.X. Jian et al., Nucl. Phys. **A503** 560 (1989)
- [4] F. Saint-Laurent et al., Phys. Lett. **B202** 190 (1988)
- [5] E. Crema et al., Phys. Lett. **B258** 266 (1991)
- [6] E. Piaseki et al., Phys. Rev. Lett. **66** 1291 (1991)
- [7] M.F. Rivet et al., Proceedings of the XXXI International Winter Meeting on Nuclear Physics, Bormio (Italy) 1993; B.Borderie, Ann. Phys. **Fr.** **17** 349 (1992)
- [8] E. Suraud, Nucl. Phys. **A462** 109 (1987); E. Suraud, C. Grégoire and B. Tamain; Progr. Part. Nucl. Phys. **23** 357 (1989)
- [9] B. Remaud, C. Grégoire, F. Sébille, and P. Schuck, Nucl. Phys. **A488** 423 (1988)
- [10] H.M. Xu, P. Danielewicz and W.G. Lynch, Phys. Lett. **B299** 199 (1993)
- [11] B. Remaud, F. Sébille, C. Grégoire, L. Vinet and Y. Raffray, Nucl. Phys. **A447** 555c (1985)
- [12] C. Grégoire, B. Remaud, F. Sébille, L. Vinet and Y. Raffray, Nucl. Phys. **A465** 317 (1987)
- [13] V. de la Mota, in preparation
- [14] D. Idier, PhD Thesis; Université de Nantes (1993)
- [15] M. Brack, C. Guet and H.-B. Håkansson, Phys. Rep. **123** 275 (1985)

- [16] C. Toepffer and Ch.Y. Wong, *Phys. Rev.* **C25** 1018 (1982)
- [17] D.T. Kohn, N. Ohtsuka, A. Faessler, M.A. Martin, S.W. Huang, E. Lehmann and Y. Lofty, *Nucl. Phys.* **A542** 671 (1992)
- [18] P. Ring and P. Schuck, *The Nuclear Many Body Problem*, (1980) Springer-Verlag NY Inc.
- [19] B. Benhassine, M. Farine, E.S. Hernández, D. Idier, B. Remaud and F. Sébille, *Nucl. Phys. A* in press
- [20] W. Cassing, *Zeit. Phys.* **A327** 447 (1987)

Figure Captions

Fig. 1. Momentum distributions of two colliding sharp Fermi spheres, separated by their relative momentum ε . k_r , k_z and k_F are the radial, longitudinal and Fermi momentum, respectively.

Fig. 2. Residue excitation energies as a function of time for the collision Ca+Ca $E/A=60$ MeV, $b=0$ Fm. These calculations are performed with two-body collisions in the local sphere (dotted line) and local bisphere (dashed line) approximations, and without collisions in the local bisphere approximation (solid line).

Figs. 3. Energy contributions as a function of time in the LBA approximation for the central Ca+Ca reaction at $E/A=60$ MeV (a) and 40 MeV (b) (see text). The dynamical calculation includes residual interactions.

Fig. 4. Relaxation times as a function of the energy in central collisions: in Ca+Ca is τ in dashed-dotted line; in Pb+Pb are τ and τ_Q in dotted and solid lines, respectively.

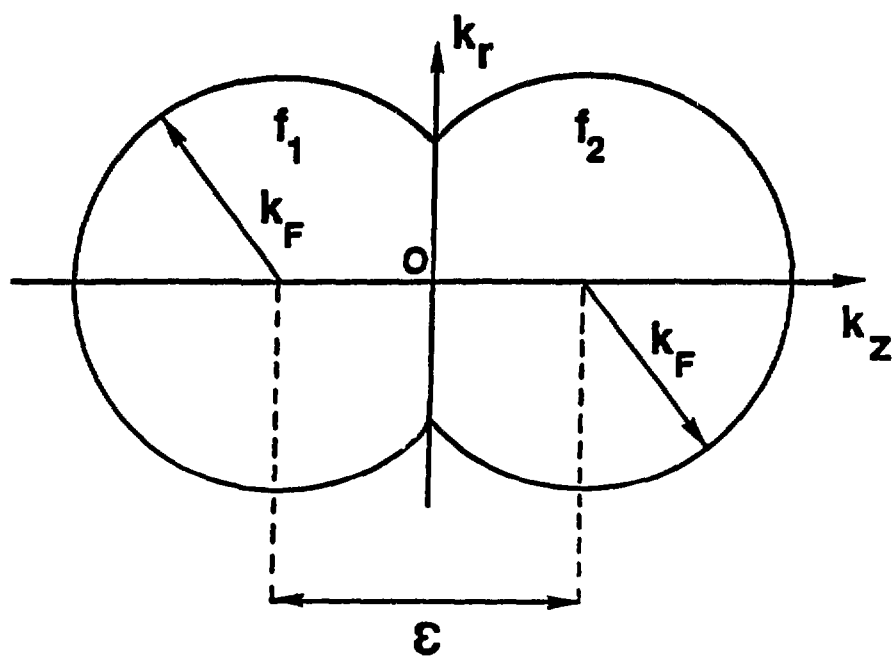


Figure 1

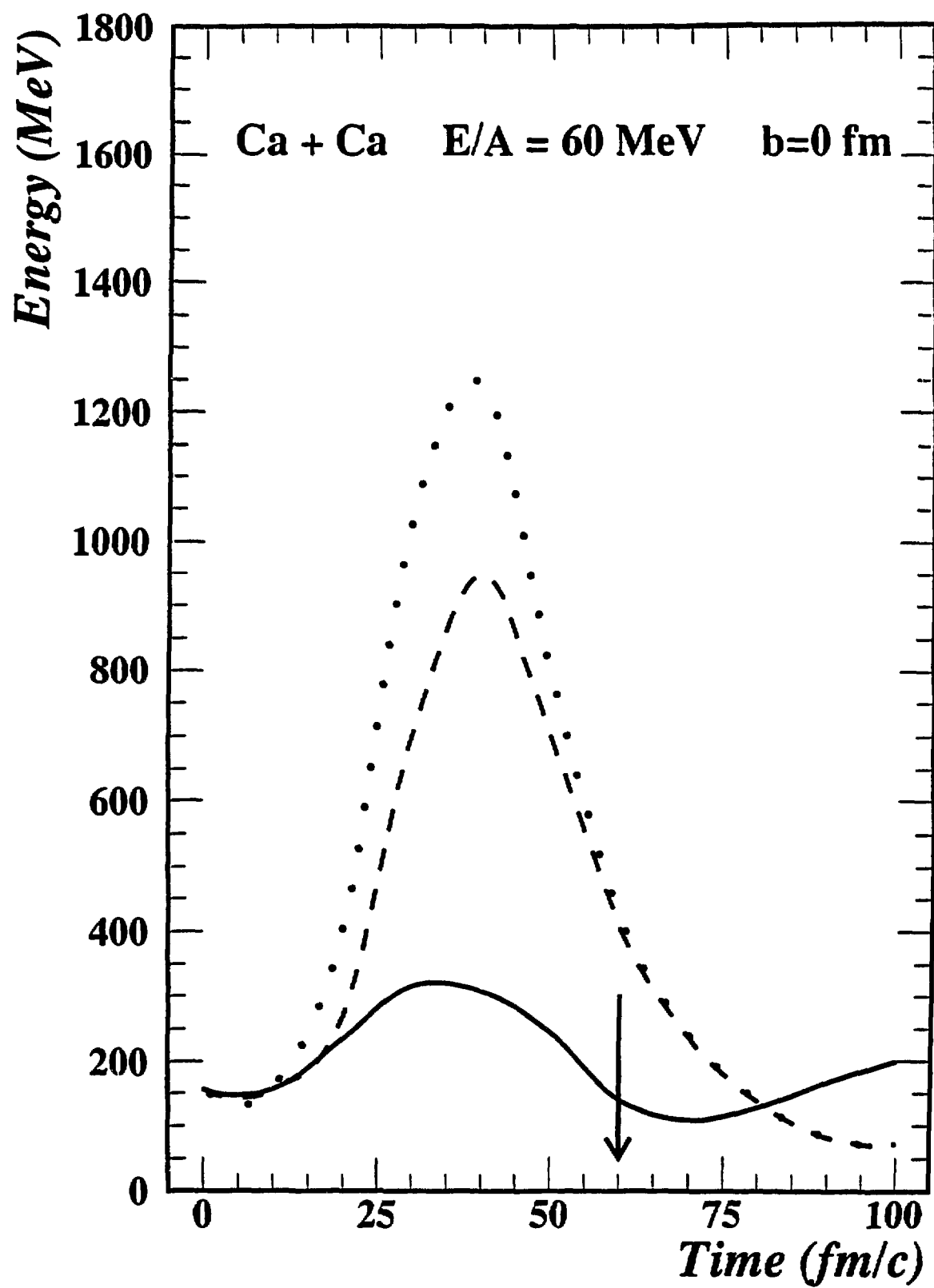


Figure 2

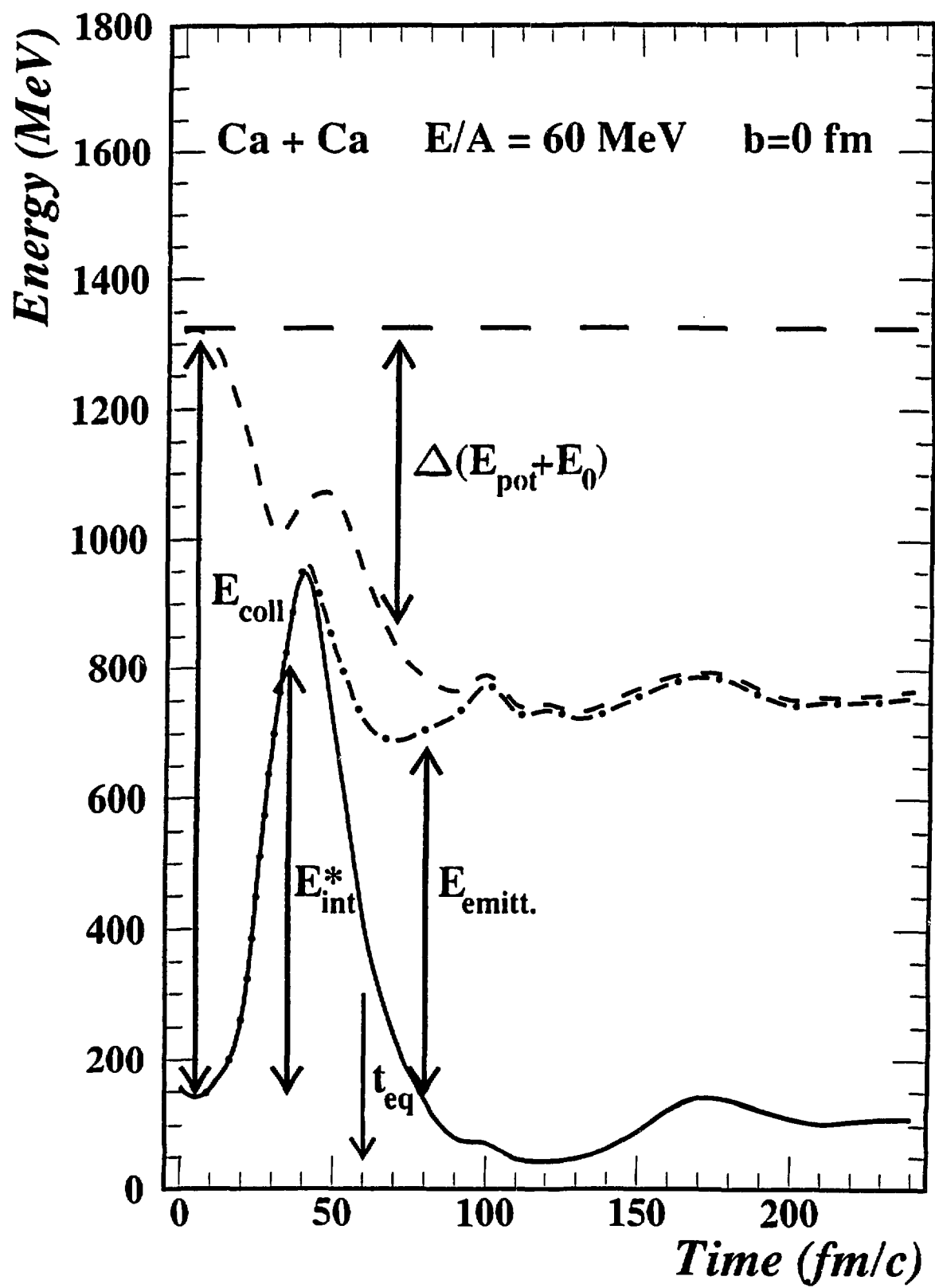


Figure 3.a

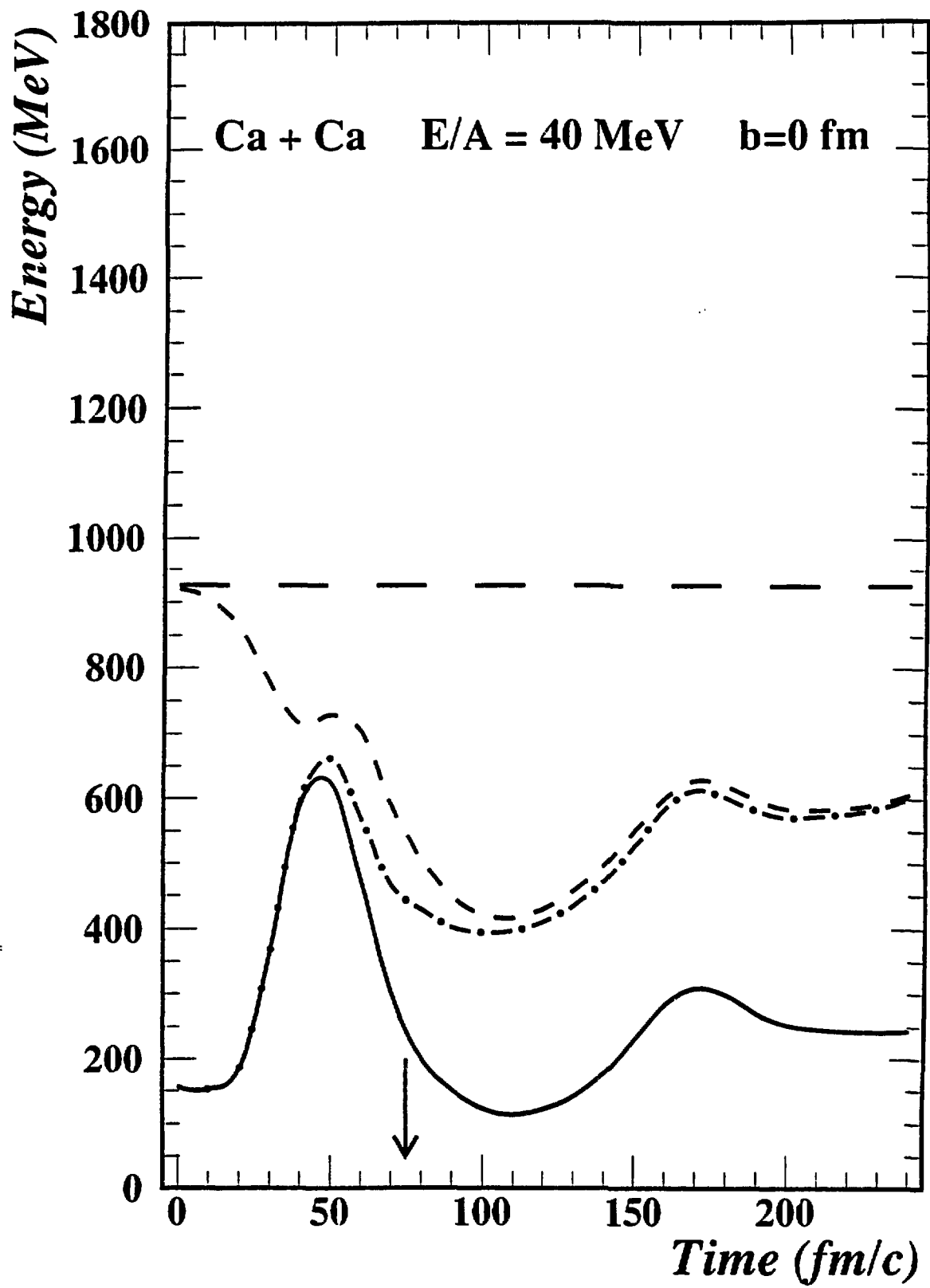


Figure 3.b

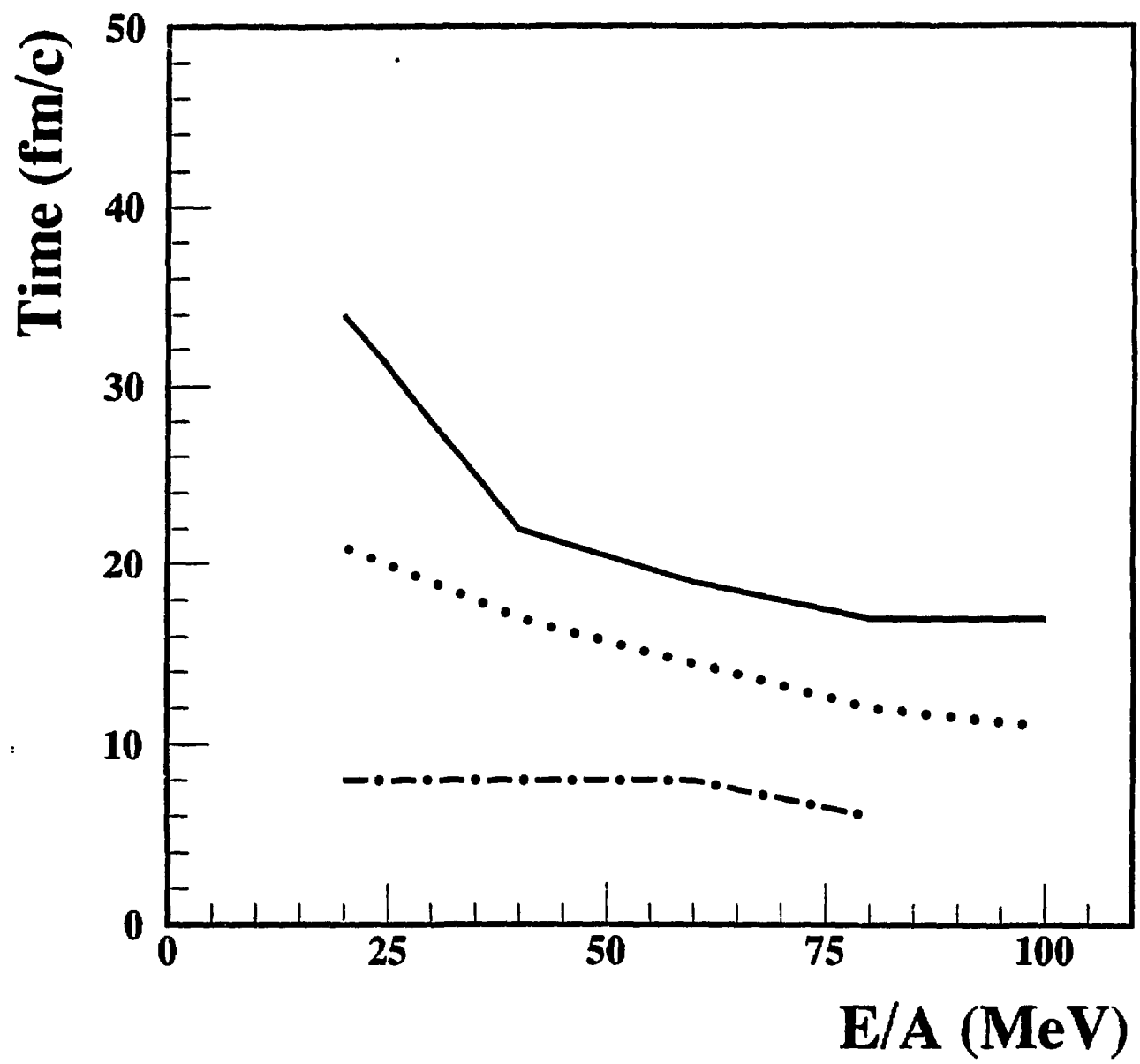


Figure 4